PATH TRACKING CONTROL BASED ON GUARANTEED STATE ESTIMATION FOR A TILT-ROTOR UAV

Brenner Santana Rego* Guilherme Vianna Raffo*

*Graduate Program in Electrical Engineering – PPGEE
Department of Electronic Engineering – DELT
Federal University of Minas Gerais – UFMG, Belo Horizonte, MG, Brazil

Email: brennersr7@ufmg.br, raffo@ufmg.br

Abstract— This paper addresses the problem of path tracking control for a tilt-rotor unmanned aerial vehicle (UAV), in the presence of external disturbances and noisy measurements. A deterministic, guaranteed state estimator based on zonotopes is proposed in this work for dealing with the available measurements. The state estimator is shown to be capable of providing full information about the states of the UAV, even when the sensors have different sampling times. Then, a discrete-time linear quadratic regulator is designed for path tracking control with constant disturbances rejection, with feedback from the estimated states. Simulation results are presented in order to validate the proposed strategy.

Keywords— UAV, Guaranteed state estimation, Sensor fusion, Path tracking.

Resumo— Este artigo trata o problema de seguimento de trajetória de um veículo aéreo não tripulado (VANT) do tipo *tilt-rotor*, na presença de perturbações externas e medições ruidosas. Um estimador de estados garantido baseado em zonotopos, determinístico, é proposto neste trabalho para lidar com as medições disponíveis. Mostra-se que o estimador de estados é capaz de fornecer informação completa sobre os estados do VANT, mesmo quando os sensores possuem diferentes períodos de amostragem. Um regulador linear quadrático, de tempo discreto, é então projetado para seguimento de trajetória com rejeição a perturbações constantes, sendo realimentado com os estados fornecidos pelo estimador. Resultados de simulação são apresentados com o objetivo de validar a estratégia proposta.

Palavras-chave— VANT, Estimação de estados garantido, Fusão sensorial, Seguimento de trajetória.

1 Introduction

Unmanned aerial vehicles (UAVs) have received great attention from researchers in the last two decades. Recently, researches focusing on the design and control of convertible UAVs have grown considerably, in which the tilt-rotor configuration is considered. Tilt-rotor UAVs are hybrid aircrafts, capable of performing high-speed flights, as fixed-wing ones, and vertical take-off and landing, as rotorcrafts. Some works concerning tilt-rotor UAVs are: Di Francesco and Mattei (2015), which proposes a controller based on incremental nonlinear dynamic inversion for a tilt-rotor UAV; and Almeida and Raffo (2015), which addresses the problem of load transportation.

The problem of state estimation often arises in state-feedback control, when incomplete state information is available for feedback connection, or, e.g., when available information is corrupted with noise. In the literature, state estimators based on stochastic approaches, like the Kalman filter, are often employed for solving this problem, by providing all the system states to the controller with minimum estimation error variance. However, in order to design these states estimators, assumptions about the probability distributions of the measurement disturbances must be made.

Guaranteed state estimation approaches, which are deterministic, are based on the construction of sets that include, with guarantee, the system states consistent with available measurements. These approaches are suitable for cases in which bounds for the measurement uncertainties are known. In the last decades, several authors have proposed guaranteed estimation techniques for discrete-time systems: Chisci et al. (1996), which presents a recursive algorithm based on parallelotopes for linear systems; and Alamo et al. (2005) and Le et al. (2013), which propose techniques based on zonotopes for nonlinear systems and for uncertain linear systems, respectively.

The present work deals with path tracking control of a tilt-rotor UAV, subject to a scenario with external disturbances and noisy measurements. Moreover, available sensors are assumed to have different sampling times. A guaranteed state estimator, based on the zonotopic technique proposed by Alamo et al. (2005), is designed in order to provide information about the entire state vector from the available measurements. The technique is adapted for multi-output systems whose measurement vector is not complete at every time instant. Thereafter, a discrete-time linear quadratic regulator is designed for the path tracking task, based on discrete-time linearized error dynamics with integral actions. The control loop is then closed by choosing the centers of the zonotopes as estimated states.

2 System modeling

This section briefly describes the dynamic model of the tilt-rotor UAV, which is obtained by Euler-

Lagrange formulation. A detailed treatment can be found in Donadel et al. (2014).

Figure 1 illustrates the tilt-rotor UAV, which is regarded as a mechanical system composed of three rigid bodies: i) main body, composed of carbon-fiber structure, landing gear, batteries and electronic devices; ii) right rotor group, which includes the right servomotor and right propeller; and iii) left rotor group, which includes the left servomotor and left propeller.

The inertial frame, the aircraft's geometric center frame, and the frame attached to the i-th rigid body's center of mass, $i \in \{1,2,3\}$, are denoted by $\mathcal{I}$, $\mathcal{B}$ and $\mathcal{C}_i$, respectively. It is assumed that the rotor groups' centers of mass are located at their respective tilting axes. The aircraft position with respect to $\mathcal{I}$ is denoted by $\boldsymbol{\xi} \triangleq [x \;\, y \;\, z]^T$, and its orientation is described by Euler angles $\boldsymbol{\eta} \triangleq [\phi \;\, \theta \;\, \psi]^T$ using the ZYX convention about local axes (Jazar, 2010). Vectors $\boldsymbol{d}^{\mathcal{B}}_{\mathcal{C}_i}$ denote displacements from $\mathcal{B}$ to $\mathcal{C}_i$. Furthermore, $\boldsymbol{R}^{\mathcal{B}}_{\mathcal{C}_1} \triangleq \boldsymbol{I}_{3\times 3}$, $\boldsymbol{R}^{\mathcal{B}}_{\mathcal{C}_2} \triangleq \boldsymbol{R}_{x,-\beta}\boldsymbol{R}_{y,\alpha_{\mathrm{R}}}$ and $\boldsymbol{R}^{\mathcal{B}}_{\mathcal{C}_3} \triangleq \boldsymbol{R}_{x,\beta}\boldsymbol{R}_{y,\alpha_{\mathrm{L}}}$, where α_{R} and α_{L} are the tilting angles, and β corresponds to a fixed inclination of the propellers towards the aircraft's geometric center, designed for improving controllability (Raffo et al., 2011).

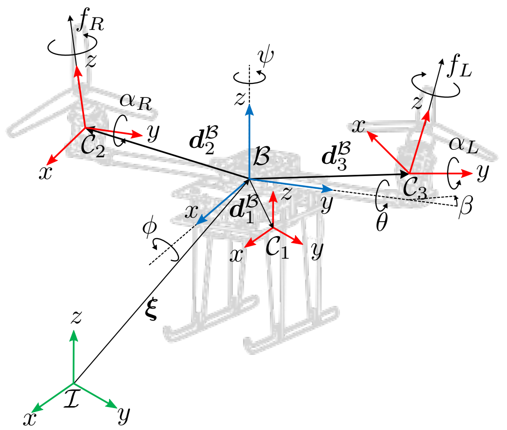

Figure 1: Tilt-rotor UAV and kinematics.

Choosing $\boldsymbol{q} \triangleq [\boldsymbol{\xi}^T \; \boldsymbol{\eta}^T \; \alpha_R \; \alpha_L]^T$ as generalized coordinates, the tilt-rotor UAV's equations of motion are written as

$$\boldsymbol{M}\ddot{\boldsymbol{q}} + \boldsymbol{C}\dot{\boldsymbol{q}} + \boldsymbol{g} = \boldsymbol{L}\boldsymbol{u} + \boldsymbol{d}, \qquad (1)$$

where $\boldsymbol{M} \triangleq \boldsymbol{M}(\boldsymbol{q})$ is the inertia matrix, $\boldsymbol{C} \triangleq \boldsymbol{C}(\boldsymbol{q},\dot{\boldsymbol{q}})$ is the Coriolis matrix obtained through Christoffel symbols of the first kind, $\boldsymbol{g} \triangleq \boldsymbol{g}(\boldsymbol{q})$ is the vector of gravitational forces, $\boldsymbol{u} \triangleq [f_R \; f_L \; \tau_{\alpha_R} \; \tau_{\alpha_L}]^T$ is the input vector (composed of thrust forces and servomotor torques), $\boldsymbol{L} \triangleq \boldsymbol{L}(\boldsymbol{q})$ maps the system inputs to generalized forces, and $\boldsymbol{d}$ is a vector of external disturbances. Moreover, defining $\boldsymbol{x} \triangleq [\boldsymbol{q}^T \; \dot{\boldsymbol{q}}^T]^T$, the dynamic equation (1) is rewritten in the state-space representation

$$\dot{\boldsymbol{x}} = \boldsymbol{f}(\boldsymbol{x},\boldsymbol{u},\boldsymbol{d}) = \begin{bmatrix} \dot{\boldsymbol{q}} \\ \boldsymbol{M}^{-1}\left[-\boldsymbol{C}\dot{\boldsymbol{q}} - \boldsymbol{g} + \boldsymbol{L}\boldsymbol{u} + \boldsymbol{d}\right] \end{bmatrix}. \qquad (2)$$

2.1 Linearized model

In addition, for control strategy purposes, system (2) is linearized through first order expansion in Taylor series around a generic time-varying trajectory, in a disturbance-free scenario, yielding to

$$\delta\dot{\boldsymbol{x}} = \boldsymbol{A}_{\mathrm{c}}(t)\delta\boldsymbol{x} + \boldsymbol{B}_{\mathrm{c}}(t)\delta\boldsymbol{u} + \boldsymbol{N}_{\mathrm{c}}(t)\boldsymbol{d}, \qquad (3)$$

where 'c' denotes continuous-time, $\delta\cdot \triangleq (\cdot) - (\cdot)^{\mathrm{tr}}$, with 'tr' denoting trajectory, and

$$\boldsymbol{A}_{\mathrm{c}}(t) = \frac{\partial \boldsymbol{f}(\boldsymbol{x},\boldsymbol{u},\boldsymbol{d})}{\partial \boldsymbol{x}}\Big|_{\substack{\boldsymbol{x}=\boldsymbol{x}^{\mathrm{tr}} \\ \boldsymbol{u}=\boldsymbol{u}^{\mathrm{tr}}}} \in \mathbb{R}^{16\times 16},$$
$$\boldsymbol{B}_{\mathrm{c}}(t) = \frac{\partial \boldsymbol{f}(\boldsymbol{x},\boldsymbol{u},\boldsymbol{d})}{\partial \boldsymbol{u}}\Big|_{\substack{\boldsymbol{x}=\boldsymbol{x}^{\mathrm{tr}} \\ \boldsymbol{u}=\boldsymbol{u}^{\mathrm{tr}}}} \in \mathbb{R}^{16\times 4},$$
$$\boldsymbol{N}_{\mathrm{c}}(t) = \frac{\partial \boldsymbol{f}(\boldsymbol{x},\boldsymbol{u},\boldsymbol{d})}{\partial \boldsymbol{d}}\Big|_{\substack{\boldsymbol{x}=\boldsymbol{x}^{\mathrm{tr}} \\ \boldsymbol{u}=\boldsymbol{u}^{\mathrm{tr}}}} \in \mathbb{R}^{16\times 8}.$$

3 Guaranteed state estimator design

This section presents the design of a state estimator based on the zonotopic guaranteed state estimation (ZSGE) technique (Alamo et al., 2005), which is capable of providing information about all states of the tilt-rotor UAV. It is assumed that available measurements are noisy and provided by sensors with different sampling times (e.g. a Global Positioning System (GPS) equipment and an Inertial Measurement Unit (IMU)). Necessary notation and definitions are introduced.

3.1 Mathematical preliminaries and the ZGSE

Let $\mathbb{IR}$ denote the set of compact real intervals $\lfloor a \rceil = [\underline{a}, \,\overline{a}] \triangleq \{a : \underline{a} \le a \le \overline{a}, \; \underline{a}, \,\overline{a} \in \mathbb{R}\}$. Then, $\mathrm{mid}\{\lfloor a \rceil\} \triangleq (1/2)(\underline{a} + \overline{a})$ and $\mathrm{diam}\{\lfloor a \rceil\} \triangleq (\overline{a} - \underline{a})$. Interval arithmetic operations are defined by $\lfloor a \rceil \odot \lfloor b \rceil \triangleq \{a \odot b : a \in \lfloor a \rceil, \, b \in \lfloor b \rceil\}$, where $\odot$ stands for any of the four basic arithmetic operations (Moore et al., 2009). Elementary functions of $\lfloor a \rceil$, such as $\sin(\lfloor a \rceil)$ and $\exp(\lfloor a \rceil)$, are defined by computing their ranges over $\lfloor a \rceil$. An interval vector (called as box) is denoted by $\lfloor \boldsymbol{a} \rceil$. An interval matrix is denoted by $\lfloor \boldsymbol{A} \rceil$. For boxes and interval matrices, $\mathrm{mid}\{\cdot\}$ and $\mathrm{diam}\{\cdot\}$ are defined component-wise. $\square\{f\}$ denotes an interval extension of f (Moore et al., 2009).

The unitary interval $[-1, \, 1]$ is denoted by $\mathbb{B}$. A r-dimensional unitary box, $\mathbb{B}^r$, is the Cartesian product of r unitary intervals. The Minkowski sum of two sets is defined by $\mathbb{X} \oplus \mathbb{Y} \triangleq \{x + y : x \in \mathbb{X}, \; y \in \mathbb{Y}\}$. A n-zonotope of order r, with center $\boldsymbol{c} \in \mathbb{R}^n$ and generator matrix $\boldsymbol{G} \in \mathbb{R}^{n\times r}$, is an affine transformation of a unitary box, defined by $\{\boldsymbol{c} + \boldsymbol{G}\boldsymbol{b} : \boldsymbol{b} \in \mathbb{B}^r\} = \boldsymbol{c} \oplus \boldsymbol{G}\mathbb{B}^r$. The Minkowski sum of two zonotopes is given by $\mathbb{Z}_1 \oplus \mathbb{Z}_2 = (\boldsymbol{c}_1 +$

$\boldsymbol{c}_2) \oplus [\boldsymbol{G}_1\ \boldsymbol{G}_2]\mathbb{B}^{r_1+r_2}$. A n-strip is defined by $\mathbb{S} \triangleq \{\boldsymbol{x} \in \mathbb{R}^n : |\boldsymbol{\rho}^T\boldsymbol{x} - \gamma| \leq \sigma\}$, with γ, $\sigma \in \mathbb{R}$, $\boldsymbol{\rho} \in \mathbb{R}^n$.

Define a family of n-zonotopes as $\mathbb{Z}_{\llcorner\urcorner} \triangleq \boldsymbol{c} \oplus {\llcorner}\boldsymbol{G}{\urcorner}\mathbb{B}^r = \{\boldsymbol{c} + \boldsymbol{G}\boldsymbol{b} : \boldsymbol{G} \in {\llcorner}\boldsymbol{G}{\urcorner}$ and $\boldsymbol{b} \in \mathbb{B}^r\}$. Then, a zonotope inclusion $\diamond\{\mathbb{Z}_{\llcorner\urcorner}\} \supseteq \mathbb{Z}_{\llcorner\urcorner}$ is defined by $\diamond\{\mathbb{Z}_{\llcorner\urcorner}\} \triangleq \boldsymbol{c} \oplus [\mathrm{mid}\{{\llcorner}\boldsymbol{G}{\urcorner}\}\ \ \boldsymbol{H}]\mathbb{B}^{n+r}$, where $\boldsymbol{H}_{ii} \triangleq (1/2)\sum_{j=1}^{r} \mathrm{diam}\{{\llcorner}\boldsymbol{G}{\urcorner}_{ij}\}$ (Alamo et al., 2005).

Consider a nonlinear discrete-time system with time update $\boldsymbol{x}_k = \boldsymbol{f}(\boldsymbol{x}_{k-1}, \boldsymbol{w}_{k-1})$ and measurement $y_k = g(\boldsymbol{x}_k, v_k)$, where $\boldsymbol{x}_k \in \mathbb{R}^{n_x}$, $y_k \in \mathbb{R}$, $\boldsymbol{w}_k \in \mathbb{R}^{n_w}$ represents external disturbances, process noise and parametric uncertainties, and $v_k \in \mathbb{R}$ represents measurement noise. Assume that $\boldsymbol{w}_k \in \mathbb{W}$, $v_k \in \mathbb{V}$ and $\boldsymbol{x}_0 \in \mathbb{X}_0$, where $\mathbb{W}$, $\mathbb{V}$ and $\mathbb{X}_0$ are known compact sets. Then, the uncertain trajectory of the system is defined by $\boldsymbol{f}(\mathbb{X}_{k-1}, \mathbb{W})$, the set of states consistent with y_k if defined as $\mathbb{X}_{y_k} \triangleq \{\boldsymbol{x} \in \mathbb{R}^{n_x} : y_k \in g(\boldsymbol{x}, \mathbb{V})\}$, and the exact uncertain state set is defined by $\mathbb{X}_k \triangleq \boldsymbol{f}(\mathbb{X}_{k-1}, \mathbb{W}) \cap \mathbb{X}_{y_k}$. The ZGSE uses zonotopes and strips in order to estimate an outer bound of the exact uncertain state set at time instant k, denoted by $\hat{\mathbb{X}}_k$.

As shown by Kühn (1998), orbits of discrete-time systems can be computed by zonotopes with reduced overestimation. Assuming that a zonotope $\hat{\mathbb{X}}_{k-1} = \boldsymbol{c}_{\hat{\boldsymbol{x}}_{k-1}} \oplus \boldsymbol{G}_{\hat{\boldsymbol{x}}_{k-1}}\mathbb{B}^{r_{\hat{\boldsymbol{x}}_{k-1}}}$ is available, and that $\mathbb{W} = \boldsymbol{c}_w \oplus \boldsymbol{G}_w\mathbb{B}^{r_w}$, an outer bound of the uncertain trajectory $\boldsymbol{f}(\hat{\mathbb{X}}_{k-1}, \mathbb{W})$ is obtained by $\bar{\mathbb{X}}_k = \mathbb{Z}_q \oplus \diamond\{{\llcorner}\boldsymbol{M}{\urcorner}\mathbb{B}^{r_x}\}$, where ${\llcorner}\boldsymbol{M}{\urcorner} \triangleq \square\{\nabla_{\boldsymbol{x}}\boldsymbol{f}(\hat{\mathbb{X}}_{k-1}, \mathbb{W})\}\boldsymbol{G}_{\hat{\boldsymbol{x}}_{k-1}}$ and $\mathbb{Z}_q \supseteq \boldsymbol{f}(\boldsymbol{c}_{\hat{\boldsymbol{x}}_{k-1}}, \mathbb{W})$. This operation is called *prediction*.

A strip $\bar{\mathbb{X}}_{y_k} \triangleq \{\boldsymbol{x} \in \mathbb{R}^{n_x} : |\boldsymbol{\rho}^T\boldsymbol{x} - y_k - s| \leq \sigma\}$ containing the set of consistent states is computed by interval arithmetic, such that $\boldsymbol{\rho} = \mathrm{mid}\{\square\{\nabla_{\boldsymbol{x}} g(\bar{\mathbb{X}}_k, \mathbb{V})\}\}$ and $\boldsymbol{\rho}^T\bar{\mathbb{X}}_k - g(\bar{\mathbb{X}}_k, \mathbb{V}) \subseteq [s-\sigma,\ s+\sigma]$. Then, a zonotope $\hat{\mathbb{X}}_k(\boldsymbol{\lambda}) = \boldsymbol{c}_{\hat{\boldsymbol{x}}_k}(\boldsymbol{\lambda}) \oplus \boldsymbol{G}_{\hat{\boldsymbol{x}}_k}(\boldsymbol{\lambda})\mathbb{B}^{r_{\hat{\boldsymbol{x}}_k}}$ containing $\bar{\mathbb{X}}_k \cap \bar{\mathbb{X}}_{y_k}$ is computed as $\boldsymbol{c}_{\hat{\boldsymbol{x}}_k}(\boldsymbol{\lambda}) = \boldsymbol{c}_{\bar{\boldsymbol{x}}_k} + \boldsymbol{\lambda}(\gamma - \boldsymbol{\rho}^T\boldsymbol{c}_{\bar{\boldsymbol{x}}_k})$ and $\boldsymbol{G}_{\hat{\boldsymbol{x}}_k}(\boldsymbol{\lambda}) = [(\boldsymbol{I}_{n_x \times n_x} - \boldsymbol{\lambda}\boldsymbol{\rho}^T)\boldsymbol{G}_{\hat{\boldsymbol{x}}_k}\ \ \sigma\boldsymbol{\lambda}]$, where $\boldsymbol{\lambda} \in \mathbb{R}^{n_x}$ is a parameter chosen by design criteria. These two operations together are called *correction*. A choice that minimizes the Frobenius norm of $\boldsymbol{G}_{\hat{\boldsymbol{x}}_k}(\boldsymbol{\lambda})$ is given by $\boldsymbol{\lambda} = (\boldsymbol{G}_{\bar{\boldsymbol{x}}_k}\boldsymbol{G}_{\bar{\boldsymbol{x}}_k}^T\boldsymbol{\rho})/(\boldsymbol{\rho}^T\boldsymbol{G}_{\bar{\boldsymbol{x}}_k}\boldsymbol{G}_{\bar{\boldsymbol{x}}_k}^T\boldsymbol{\rho} + \sigma^2)$.

The ZGSE is summarized in Algorithm 1.

Algorithm 1 ZGSE algorithm

1: Compute the zonotope $\bar{\mathbb{X}}_k \supseteq \boldsymbol{f}(\hat{\mathbb{X}}_{k-1}, \mathbb{W})$
2: Compute the strip $\bar{\mathbb{X}}_{y_k} \supseteq \mathbb{X}_{y_k}$
3: Compute the zonotope $\hat{\mathbb{X}}_k(\boldsymbol{\lambda}) \supseteq \bar{\mathbb{X}}_k \cap \bar{\mathbb{X}}_{y_k}$

The order of $\hat{\mathbb{X}}_k$ increases at each time step. Algorithm 2 can be used for establishing an upper limit s to it.

Note that the ZGSE is formulated for single-output systems. In the case of multi-output systems, steps 2 and 3 from Algorithm 1 can be applied iteratively for each element of the measurement vector (Le et al., 2013).

Algorithm 2 Zonotope order reduction

$\boldsymbol{H} \leftarrow$ columns of $\boldsymbol{G}_{\hat{\boldsymbol{x}}_k}$ ordered in decreasing Euclidean norm
$\boldsymbol{H}_T \leftarrow$ first $s - n_x$ columns of $\boldsymbol{H}$
for $i = 1, ..., n$ **do**
  $\boldsymbol{Q}_{ii} \leftarrow \sum_{j=s-n_x+1}^{r_{\hat{\boldsymbol{x}}_k}} |\boldsymbol{H}_{ij}|$
end for
$\hat{\mathbb{X}}_k \leftarrow \boldsymbol{c}_{\hat{\boldsymbol{x}}_k} \oplus [\boldsymbol{H}_T\ \boldsymbol{Q}]\mathbb{B}^s$

3.2 State estimator for the tilt-rotor UAV

Although the ZGSE is formulated for nonlinear systems, computational complexity arises when performing the prediction operation, for the time update equation obtained by discretizing (2). Then, equations (3) are used instead, evaluated at an equilibrium point, and discretized using the zero-order-holder (ZOH) method, leading to[1]

$$\Delta\boldsymbol{x}_k = \boldsymbol{A}_{\mathrm{d}}\Delta\boldsymbol{x}_{k-1} + \boldsymbol{B}_{\mathrm{d}}\Delta\boldsymbol{u}_{k-1} + \boldsymbol{N}_{\mathrm{d}}\boldsymbol{d}_{k-1} + \boldsymbol{w}_{k-1}, \quad (4)$$

where ‘d’ denotes ‘discrete-time’, $\boldsymbol{A}_{\mathrm{d}} \in \mathbb{R}^{16\times16}$, $\boldsymbol{B}_{\mathrm{d}} \in \mathbb{R}^{16\times4}$, $\boldsymbol{N}_{\mathrm{d}} \in \mathbb{R}^{16\times8}$, and $\boldsymbol{w}$ represents modeling errors resulting from linearization.

This work assumes that the measurement vector is given by $\boldsymbol{y} \triangleq [\boldsymbol{q}^T\ \ \dot{\boldsymbol{\eta}}^T\ \ \dot{\alpha}_{\mathrm{R}}\ \ \dot{\alpha}_{\mathrm{L}}]^T$, however not all elements are available at every instant k. As a function of $\boldsymbol{x}_k$, we have $\boldsymbol{y}_k = \boldsymbol{H}_{\mathrm{d}}\boldsymbol{x}_k + \boldsymbol{v}_k$, where $\boldsymbol{H}_{\mathrm{d}} \in \mathbb{R}^{13\times16}$ and $\boldsymbol{v}$ is the measurement noise. Rewriting it as a function of $\Delta\boldsymbol{x}$ yields $\boldsymbol{y}_k = \boldsymbol{H}_{\mathrm{d}}\Delta\boldsymbol{x}_k + \bar{\boldsymbol{v}}_k$, where $\bar{\boldsymbol{v}}_k \triangleq \boldsymbol{H}_{\mathrm{d}}\boldsymbol{x}^{\mathrm{eq}} + \boldsymbol{v}_k$.

Furthermore, assume that[2] $\boldsymbol{d} = [\bar{\boldsymbol{d}}\ \ \boldsymbol{0}_{1\times5}]^T$, $\bar{\boldsymbol{d}} \in \mathbb{R}^3$, and define $\tilde{\boldsymbol{d}}_{k-1} \triangleq \bar{\boldsymbol{d}}_k - \bar{\boldsymbol{d}}_{k-1}$. In order to estimate the external disturbances along with the system states, an augmented state vector $\boldsymbol{\nu} \triangleq [\Delta\boldsymbol{x}^T\ \ \ \bar{\boldsymbol{d}}^T]^T$ is introduced, yielding

$$\begin{aligned}\boldsymbol{\nu}_k &= \boldsymbol{A}_{\boldsymbol{\nu}}\boldsymbol{\nu}_{k-1} + \boldsymbol{B}_{\boldsymbol{\nu}}\Delta\boldsymbol{u}_{k-1} + \bar{\boldsymbol{w}}_{k-1},\\ \boldsymbol{y}_k &= \boldsymbol{H}_{\boldsymbol{\nu}}\boldsymbol{\nu}_k + \bar{\boldsymbol{v}}_k,\end{aligned} \quad (5)$$

where

$$\boldsymbol{A}_{\boldsymbol{\nu}} = \begin{bmatrix}\boldsymbol{A}_{\mathrm{d}} & \bar{\boldsymbol{N}}_{\mathrm{d}}\\ \boldsymbol{0}_{3\times16} & \boldsymbol{I}_{3\times3}\end{bmatrix} \in \mathbb{R}^{19\times19}, \quad \boldsymbol{B}_{\boldsymbol{\nu}} = \begin{bmatrix}\boldsymbol{B}_{\mathrm{d}}\\ \boldsymbol{0}_{3\times4}\end{bmatrix} \in \mathbb{R}^{19\times4},$$
$$\boldsymbol{H}_{\boldsymbol{\nu}} = \begin{bmatrix}\boldsymbol{H}_{\mathrm{d}} & \boldsymbol{0}_{13\times3}\end{bmatrix} \in \mathbb{R}^{13\times19}, \quad \bar{\boldsymbol{w}} \triangleq \begin{bmatrix}\boldsymbol{w}^T & \tilde{\boldsymbol{d}}^T\end{bmatrix},$$

in which $\bar{\boldsymbol{N}}_{\mathrm{d}}$ corresponds to the first three columns of $\boldsymbol{N}_{\mathrm{d}}$. The observability matrix for pair $(\boldsymbol{A}_{\boldsymbol{\nu}}, \boldsymbol{H}_{\boldsymbol{\nu}})$ is full column rank, thus (5) is observable.

Assume that $\bar{\boldsymbol{w}}$ and $\bar{\boldsymbol{v}}$ belong to compact sets represented by zonotopes $\bar{\mathbb{W}} = \boldsymbol{c}_{\bar{w}} \oplus \boldsymbol{G}_{\bar{w}}\mathbb{B}^{r_{\bar{w}}}$ and $\bar{\mathbb{V}} = \boldsymbol{c}_{\bar{v}} \oplus \boldsymbol{G}_{\bar{v}}\mathbb{B}^{r_{\bar{v}}}$, and let $\boldsymbol{\nu}_{k-1} \in \hat{\mathbb{X}}_{k-1} = \boldsymbol{c}_{\hat{x}_{k-1}} \oplus \boldsymbol{G}_{\hat{x}_{k-1}}\mathbb{B}^{r_{\hat{x}_{k-1}}}$. Furthermore, denote $\mathbb{I}_k$ as the set of available measurements at time instant k. Then, applying the ZGSE to (5) results in Algorithm 3, in which an iterative procedure was introduced in order to use all $i \in \mathbb{I}_k$, (i) denotes i-th row, and (i, j) denotes i-th row and j-th column. Since it is based on the ZGSE, and providing that $\bar{\mathbb{W}}$ contains all linearization error effects, it is guaranteed that $\boldsymbol{\nu}_k \in \hat{\mathbb{X}}_k$.

[1] To avoid misleading, for the state estimator, $(\cdot)^{\mathrm{tr}} \triangleq (\cdot)^{\mathrm{eq}}$, with ‘eq’ denoting equilibrium, and $\delta(\cdot) \triangleq \Delta(\cdot)$.

[2] It is assumed that the system is affected only by forces

Algorithm 3 Guaranteed state estimator for (5)

$\bar{\mathbb{X}}_k \leftarrow (\boldsymbol{A}_{\boldsymbol{\nu}} \boldsymbol{c}_{\hat{x}_{k-1}} + \boldsymbol{B}_{\boldsymbol{\nu}} \Delta \boldsymbol{u} + \boldsymbol{c}_{\bar{w}}) \oplus [\boldsymbol{G}_{\bar{w}} \;\; \boldsymbol{A}_{\boldsymbol{\nu}} \boldsymbol{G}_{\hat{x}_{k-1}}] \mathbb{B}^{r_{\bar{x}_k}}$
$\tilde{\mathbb{X}}_k \leftarrow \bar{\mathbb{X}}_k$
for all $i \in \mathbb{I}_k$ **do**
  $\bar{\mathbb{X}}_{\boldsymbol{y}_k(i)} \leftarrow \{\boldsymbol{x} \in \mathbb{R}^{19} : |\boldsymbol{\rho}_i^T \boldsymbol{x} - \boldsymbol{y}_k(i) - s_i| \leq \sigma_i\}$, with $\boldsymbol{\rho}_i = \boldsymbol{H}_{\boldsymbol{\nu}}(i)^T$, $s_i = -\boldsymbol{c}_{\bar{v}}(i)$, $\sigma_i = -\sum_{j=1}^{r_{\bar{v}}} |\boldsymbol{G}_{\bar{v}}(i,j)|$
  $\tilde{\mathbb{X}}_k \leftarrow (\boldsymbol{c}_{\tilde{x}_k} + \boldsymbol{\lambda}_i(\boldsymbol{y}_k(i) + s_i - \boldsymbol{\rho}_i^T \boldsymbol{c}_{\tilde{x}_k})) \oplus \boldsymbol{G}_i \mathbb{B}^{r_{\tilde{x}_k}+1}$, where $\boldsymbol{G}_i = [(\boldsymbol{I}_{19\times 19} - \boldsymbol{\lambda}_i \boldsymbol{\rho}_i^T)\boldsymbol{G}_{\tilde{x}_k} \;\; \sigma_i \boldsymbol{\lambda}_i]$ and $\boldsymbol{\lambda}_i = (\boldsymbol{G}_{\tilde{x}_k} \boldsymbol{G}_{\tilde{x}_k}^T \boldsymbol{\rho}_i)/(\boldsymbol{\rho}_i^T \boldsymbol{G}_{\tilde{x}_k} \boldsymbol{G}_{\tilde{x}_k}^T \boldsymbol{\rho}_i + \sigma_i^2)$
end for
$\hat{\mathbb{X}}_k \leftarrow \tilde{\mathbb{X}}_k$

4 Control design

This section presents the design of a discrete-time linear quadratic regulator (DLQR) for solving the path tracking problem for the tilt-rotor UAV, with constant disturbances rejection. The controller is designed based on discrete-time linearized error dynamics with integral actions.

4.1 Discrete-time linearized error dynamics

The tilt-rotor UAV is an underactuated mechanical system with only four control inputs, which means that four variables can be chosen to be regulated. In this case: x, y, z and ψ. Define $\boldsymbol{\xi}^{\mathrm{tr}} \triangleq [x^{\mathrm{tr}} \;\; y^{\mathrm{tr}} \;\; z^{\mathrm{tr}}]^T$, $\boldsymbol{\eta}^{\mathrm{tr}} \triangleq [\phi^{\mathrm{eq}} \;\; \theta^{\mathrm{eq}} \;\; \psi^{\mathrm{tr}}]^T$ and $\boldsymbol{q}^{\mathrm{tr}} \triangleq [\boldsymbol{\xi}^{\mathrm{tr}} \;\; \boldsymbol{\eta}^{\mathrm{tr}} \;\; {\alpha_{\mathrm{R}}}^{\mathrm{eq}} \;\; {\alpha_{\mathrm{L}}}^{\mathrm{eq}}]^T$. Assuming that ψ^{tr} is constant, we have $\dot{\boldsymbol{q}}^{\mathrm{tr}} = [(\dot{\boldsymbol{\xi}}^{\mathrm{tr}})^T \;\; \boldsymbol{0}_{1\times 5}]^T$ and $\ddot{\boldsymbol{q}}^{\mathrm{tr}} = [(\ddot{\boldsymbol{\xi}}^{\mathrm{tr}})^T \;\; \boldsymbol{0}_{1\times 5}]^T$. Then, define $\boldsymbol{x}^{\mathrm{tr}} \triangleq [(\boldsymbol{q}^{\mathrm{tr}})^T \;\; (\dot{\boldsymbol{q}}^{\mathrm{tr}})^T]^T$ and $\boldsymbol{u}^{\mathrm{tr}} \triangleq [f_{\mathrm{R}}^{\mathrm{tr}} \;\; f_{\mathrm{L}}^{\mathrm{tr}} \;\; \tau_{\alpha_{\mathrm{R}}}^{\mathrm{tr}} \;\; \tau_{\alpha_{\mathrm{L}}}^{\mathrm{tr}}]^T$. Evaluating (3) at these variables yields to $\delta\dot{\boldsymbol{x}} = \boldsymbol{A}_{\mathrm{c}}(t)\delta\boldsymbol{x} + \boldsymbol{B}_{\mathrm{c}}\delta\boldsymbol{u} + \boldsymbol{N}_{\mathrm{c}}\boldsymbol{d}$, where $\boldsymbol{A}_{\mathrm{c}}(t)$ is time-varying due to $\boldsymbol{u}^{\mathrm{tr}}$ (Donadel et al., 2014). For control design purposes, this work assumes that $\boldsymbol{A}_{\mathrm{c}}(t) \approx \boldsymbol{A}_{\mathrm{c}}(t)|_{\boldsymbol{u}^{\mathrm{tr}}=\boldsymbol{u}^{\mathrm{eq}}} \triangleq \boldsymbol{A}_{\mathrm{c}}$, which is constant. The subsequent error is considered as unmodeled dynamics, and the controller to be designed is assumed to be robust enough to deal with it. Therefore, $\delta\dot{\boldsymbol{x}} = \boldsymbol{A}_{\mathrm{c}}\delta\boldsymbol{x} + \boldsymbol{B}_{\mathrm{c}}\delta\boldsymbol{u} + \boldsymbol{N}_{\mathrm{c}}\boldsymbol{d}$.

For constant disturbances rejection purposes, state augmentation $\boldsymbol{\chi} \triangleq [\delta\boldsymbol{x}^T \;\; \int \delta\boldsymbol{\xi}^T \;\; \int \delta\psi]^T$ is performed, whose continuous-time dynamics are obtained by properly augmenting $\boldsymbol{A}_c$, $\boldsymbol{B}_c$ and $\boldsymbol{N}_c$. Finally, applying the ZOH discretization method over the continuous-time dynamics of $\boldsymbol{\chi}$ yields to

$$\boldsymbol{\chi}_{k+1} = \boldsymbol{A}_{\boldsymbol{\chi}}\boldsymbol{\chi}_k + \boldsymbol{B}_{\boldsymbol{\chi}}\delta\boldsymbol{u}_k + \boldsymbol{N}_{\boldsymbol{\chi}}\boldsymbol{d}_k, \qquad (6)$$

with $\boldsymbol{A}_{\boldsymbol{\chi}} \in \mathbb{R}^{20\times 20}$, $\boldsymbol{B}_{\boldsymbol{\chi}} \in \mathbb{R}^{20\times 4}$ and $\boldsymbol{N}_{\boldsymbol{\chi}} \in \mathbb{R}^{20\times 8}$. The controllability matrix for pair $(\boldsymbol{A}_{\boldsymbol{\chi}}, \boldsymbol{B}_{\boldsymbol{\chi}})$ is full row rank, thus (6) is controllable.

4.2 Discrete-time linear quadratic regulator

A DLQR for (6) is a controller that minimizes the infinite-horizon cost functional

$$\varphi_{\mathrm{DLQR}} = \sum_{k=0}^{\infty} \boldsymbol{\chi}_k^T \boldsymbol{\Omega}_{\boldsymbol{\chi}} \boldsymbol{\chi}_k + \delta\boldsymbol{u}_k^T \boldsymbol{\Omega}_{\boldsymbol{u}} \delta\boldsymbol{u}_k,$$

applied to the UAV's geometric center.

where $\boldsymbol{\Omega}_{\boldsymbol{\chi}} \in \mathbb{R}^{20\times 20}$ and $\boldsymbol{\Omega}_{\boldsymbol{u}} \in \mathbb{R}^{4\times 4}$ are positive definite weighting matrices that are chosen by design criteria. It is well known (Anderson and Moore, 1989) that this optimal control problem leads to the state-feedback control law $\delta\boldsymbol{u}_k = -\boldsymbol{K}\boldsymbol{\chi}_k$, where $\boldsymbol{K} = (\boldsymbol{\Omega}_{\boldsymbol{u}} + \boldsymbol{B}_{\boldsymbol{\chi}}^T \boldsymbol{F} \boldsymbol{B}_{\boldsymbol{\chi}})^{-1}(\boldsymbol{B}_{\boldsymbol{\chi}}^T \boldsymbol{F} \boldsymbol{A}_{\boldsymbol{\chi}}) \in \mathbb{R}^{4\times 20}$, and $\boldsymbol{F} \in \mathbb{R}^{4\times 20}$ is the solution of the algebraic Riccati equation $\boldsymbol{F} = \boldsymbol{\Omega}_{\boldsymbol{\chi}} + \boldsymbol{A}_{\boldsymbol{\chi}}^T \boldsymbol{F} \boldsymbol{A}_{\boldsymbol{\chi}} - (\boldsymbol{B}_{\boldsymbol{\chi}}^T \boldsymbol{F} \boldsymbol{A}_{\boldsymbol{\chi}})^T (\boldsymbol{R} + \boldsymbol{B}_{\boldsymbol{\chi}}^T \boldsymbol{F} \boldsymbol{B}_{\boldsymbol{\chi}})^{-1} (\boldsymbol{B}_{\boldsymbol{\chi}}^T \boldsymbol{F} \boldsymbol{A}_{\boldsymbol{\chi}})$.

Moreover, a feed-forward term $\boldsymbol{u}_k^{\mathrm{tr}} = (\boldsymbol{L}_k^{\mathrm{tr}})^{+}\,[\boldsymbol{M}_k^{\mathrm{tr}} \ddot{\boldsymbol{q}}_k^{\mathrm{tr}} + \boldsymbol{C}_k^{\mathrm{tr}} \dot{\boldsymbol{q}}_k^{\mathrm{tr}} + \boldsymbol{g}_k^{\mathrm{tr}}]$ is introduced, in which $\boldsymbol{M}_k^{\mathrm{tr}} \triangleq \boldsymbol{M}(\boldsymbol{q}_k^{\mathrm{tr}})$, $\boldsymbol{C}_k^{\mathrm{tr}} \triangleq \boldsymbol{C}(\boldsymbol{q}_k^{\mathrm{tr}}, \dot{\boldsymbol{q}}_k^{\mathrm{tr}})$, $\boldsymbol{g}_k^{\mathrm{tr}} \triangleq \boldsymbol{g}(\boldsymbol{q}_k^{\mathrm{tr}})$ and $\boldsymbol{L}_k^{\mathrm{tr}} \triangleq \boldsymbol{L}(\boldsymbol{q}_k^{\mathrm{tr}})$. Furthermore, $(\boldsymbol{L}_k^{\mathrm{tr}})^{+}$ denotes the left pseudo-inverse of $\boldsymbol{L}_k^{\mathrm{tr}}$. The complete control law applied to (2) is then given by $\boldsymbol{u}_k = \boldsymbol{u}_k^{\mathrm{tr}} + \delta\boldsymbol{u}_k = \boldsymbol{u}_k^{\mathrm{tr}} - \boldsymbol{K}\boldsymbol{\chi}_k$. Note that, as $\boldsymbol{u}_k^{\mathrm{tr}}$ is computed using a left pseudo-inverse, it is not an exact solution for (2). The resulting error is also considered as unmodeled dynamics.

5 Simulation results

The model parameters of the tilt-rotor UAV, presented in Donadel (2015), resulted in the following equilibrium used to derive system (4):

$$\begin{aligned}\boldsymbol{q}^{\mathrm{eq}} = [&\boldsymbol{0}_{3\times 1} \;\; -0.00009533 \;\; 0.09440420 \;\; 0 \\ &-0.09396720 \;\; -0.09412678]^T, \quad \dot{\boldsymbol{q}}^{\mathrm{eq}} = \boldsymbol{0}_{8\times 1}, \\ \boldsymbol{u}^{\mathrm{eq}} = [&8.43564168 \;\; 8.45417328 \;\; 0 \;\; 0]^T.\end{aligned}$$

This work assumes that the available measurements are provided by a GPS, a Barometer, an IMU and sensors embedded at the servomotors. The associated parameters are shown in Table 1, in which noise from the servos' sensors have zero-mean uniform distribution, and noise from the other sensors have zero-mean Gaussian distribution. For the latter, "noise bound" means three times the standard deviation. The set $\mathbb{I}_k$ is given by the union of sets $\mathbb{I}$ of sensors whose measurements are available at time instant k.

Table 1: Sensors parameters

Sensor	$\mathbb{I}$	Noise bound	Sampling
GPS	$1, 2$	$\pm 0.15\,\mathrm{m}$	120 ms
Barometer	3	$\pm 0.51\,\mathrm{m}$	12 ms
IMU	$4, 5, 6$	$\pm 5.15\cdot 10^{-3}\,\mathrm{rad}$	12 ms
	$9, 10, 11$	$\pm 5.15\cdot 10^{-3}\,\mathrm{rad/s}$	
Servos	$7, 8$	$\pm 5.67\cdot 10^{-3}\,\mathrm{rad}$	12 ms
	$12, 13$	$\pm 0.50772\,\mathrm{rad/s}$	

For the guaranteed state estimator, system (4) was obtained for sampling time 12 ms, and it was assumed that $\bar{\mathbb{X}}_0 = [(\boldsymbol{\xi}_0^{\mathrm{tr}})^T \;\; \boldsymbol{0}_{1\times 16}]^T \oplus \boldsymbol{G}_{\bar{x}_0}\mathbb{B}^{19}$, $\bar{\mathbb{W}} = \boldsymbol{0}_{19\times 1} \oplus \boldsymbol{G}_{\bar{w}}\mathbb{B}^{19}$ and $\bar{\mathbb{V}} = \boldsymbol{H}_{\mathrm{d}}\boldsymbol{x}^{\mathrm{eq}} \oplus \boldsymbol{G}_{\bar{v}}\mathbb{B}^{13}$,

$$\begin{aligned}\boldsymbol{G}_{\bar{x}_0} =& \mathrm{diag}(0.5\cdot\boldsymbol{1}_{3\times 1}, 0.2\cdot|\phi^{\mathrm{eq}}|, 0.2\cdot|\theta^{\mathrm{eq}}|, \pi/180, \\ & 0.2\cdot|{\alpha_{\mathrm{R}}}^{\mathrm{eq}}|, 0.2\cdot|{\alpha_{\mathrm{L}}}^{\mathrm{eq}}|, 0.02\cdot\boldsymbol{1}_{11\times 1}), \\ \boldsymbol{G}_{\bar{w}} =& \mathrm{diag}(10^{-4}\cdot\boldsymbol{1}_{16\times 1}, 0.1, 0.1, 0.2), \\ \boldsymbol{G}_{\bar{v}} =& \mathrm{diag}(0.15\cdot\boldsymbol{1}_{2\times 1}, 0.51, 5.15\cdot 10^{-3}\cdot\boldsymbol{1}_{3\times 1}, \\ & 5.67\cdot 10^{-3}\cdot\boldsymbol{1}_{2\times 1}, 5.15\cdot 10^{-3}\cdot\boldsymbol{1}_{3\times 1}, 0.50772\cdot\boldsymbol{1}_{2\times 1}),\end{aligned}$$

in which $\boldsymbol{G}_{\bar{w}}$ was adjusted heuristically, and $\mathbf{1}_{\cdot\times\cdot}$ denotes a matrix of 1's.

The DLQR was designed for sampling time 12 ms. The Bryson's method (Johnson and Grimble, 1987) was used as starting point for choosing the weighting matrices, which are given by

$$\begin{aligned}\boldsymbol{\Omega_x} = \mathrm{diag}(&5, 5, 5, 4/\pi^2, 4/\pi^2, 15/\pi^2, 0.04/\pi^2, 0.04/\pi^2,\\ &1/4, 1/4, 1/4, 5/(9\pi^2), 5/(9\pi^2), 16/\pi^2,\\ &0.01/(9\pi^2), 0.01/(9\pi^2), 30, 30, 30, 0.5),\end{aligned}$$

$$\boldsymbol{\Omega_u} = \mathrm{diag}(50/(15 - f_{\mathrm{R}}^{\mathrm{eq}})^2, 50/(15 - f_{\mathrm{L}}^{\mathrm{eq}})^2, 1250, 1250),$$

where $f_{\mathrm{R}}^{\mathrm{eq}}$ and $f_{\mathrm{L}}^{\mathrm{eq}}$ are values from equilibrium $\boldsymbol{u}^{\mathrm{eq}}$.

The control loop was closed using the first 16 elements of $\boldsymbol{c}_{\hat{x}_k}$, as $\delta\boldsymbol{x} = (\boldsymbol{c}_{\hat{x}_k}(1, 2, \ldots, 16) + \boldsymbol{x}^{\mathrm{eq}}) - \boldsymbol{x}^{\mathrm{tr}}$. Moreover, the order of $\hat{\mathbb{X}}_k$ was limited to fifty times its dimension.

The trajectory to be performed is defined by the following equations: $x^{\mathrm{tr}}(t) = 4\cos(\pi t/40)$; $y^{\mathrm{tr}}(t) = 4\sin(\pi t/40)$; $z^{\mathrm{tr}}(t) = 17 - 16\cos(\pi t/40)$; and $\psi^{\mathrm{tr}} = 0$. The initial states are $\boldsymbol{x}_0 = [3.9 \quad 0.1 \quad 0.9 \quad (\boldsymbol{\eta}^{\mathrm{tr}})^T \quad \alpha_{\mathrm{R}}{}^{\mathrm{eq}} \quad \alpha_{\mathrm{L}}{}^{\mathrm{eq}} \quad \mathbf{0}_{1\times 8}]^T$.

Figure 2 shows the desired trajectory and the performed trajectory. Figure 3 shows the applied external disturbances, and Figure 4 shows the error of the regulated states. Note that, despite noise, external disturbances and multiple sampling times, the path tracking is performed with almost null steady-state error, presenting good performance of the designed DLQR controller and the guaranteed state estimator.

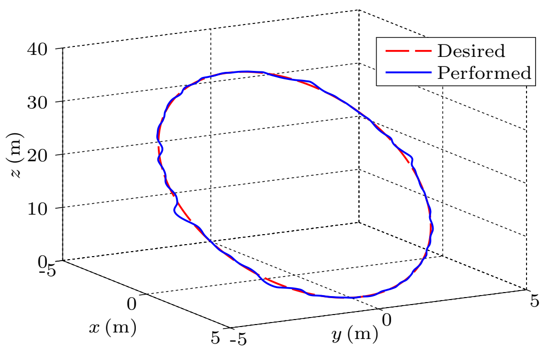

Figure 2: Desired and performed trajectories.

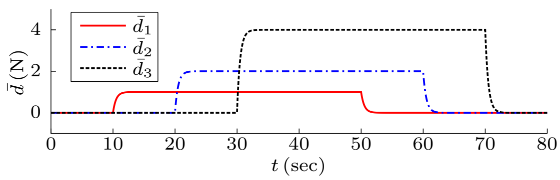

Figure 3: Applied external disturbances.

The time evolution of the remaining states is illustrated in Figures 5 and 6. These variables remain stable throughout the trajectory tracking. Figure 7 shows the computed control signals.

Estimation error and confidence limits (which are obtained by multiplying $\boldsymbol{G}_{\hat{\boldsymbol{x}}_k}\mathbb{B}^{r_{\hat{\boldsymbol{x}}_k}}$ using interval arithmetic) for x, y, $\dot{x}$ and $\dot{y}$, are shown in

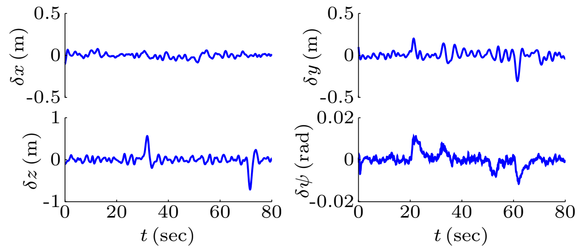

Figure 4: Error over the regulated states.

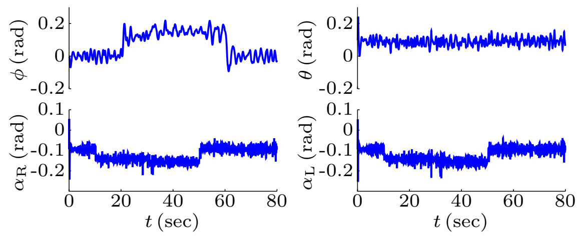

Figure 5: Time evolution of the remaining DOF.

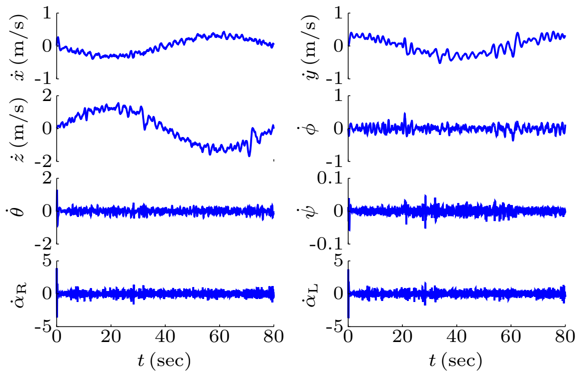

Figure 6: Velocities. Variables without specified units are given in rad/s.

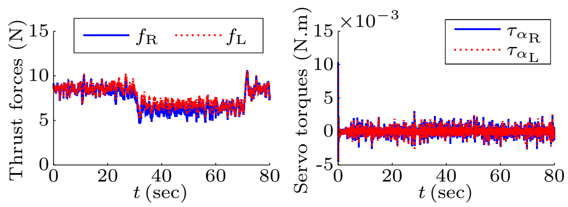

Figure 7: Control signals.

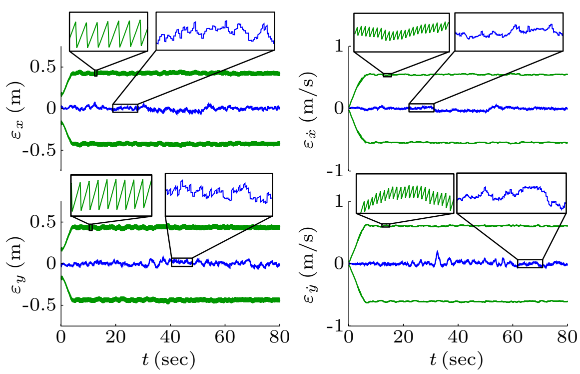

Figure 8: Estimation error of x, y, $\dot{x}$ and $\dot{y}$. Outer lines are confidence limits.

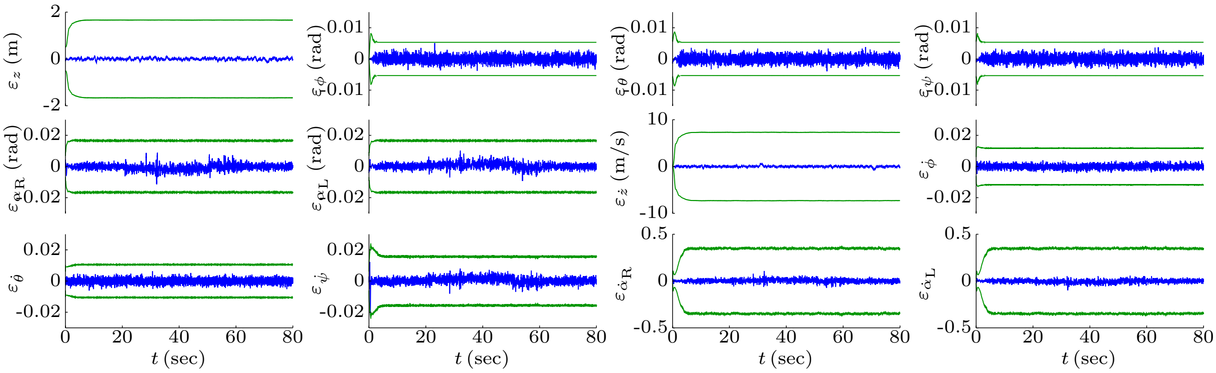

Figure 9: Estimation error of the remaining states. Outer lines are confidence limits. Variables without specified units are given in rad/s.

Figure 8. Note the "toothed" pattern of the limits, which is a consequence of the GPS sampling time. Figure 9 shows the estimation error and confidence limits for the remaining states.

6 Conclusions

This paper presented path tracking control strategy based on guaranteed state estimation for a tilt-rotor UAV. The aircraft's equations of motion were presented. Assuming that available information is provided by noisy measurements with different sampling times, a guaranteed state estimator based on zonotopes was designed, providing information about the entire state vector at the controller sampling time. Based on the discrete-time linearized error dynamics with integral actions, a DLQR was designed for path tracking with constant disturbances rejection capability. Simulation results corroborated the validity of the control strategy, and also showed the good performance of the guaranteed state estimator.

7 Acknowledgement

The authors would like to thank the Brazilian research agencies CAPES, CNPq and FAPEMIG for their financial contribution for the accomplishment of this work.

References

Alamo, T., Bravo, J. and Camacho, E. (2005). Guaranteed state estimation by zonotopes, *Automatica* **41**(6): 1035–1043.

Almeida, M. M. and Raffo, G. V. (2015). Nonlinear control of a tiltrotor uav for load transportation, *11th IFAC Symposium on Robot Control*, pp. 234–239.

Anderson, B. D. and Moore, J. B. (1989). *Optimal Control: Linear Quadratic Methods*, Prentice Hall, Englewood Cliffs, New Jersey, USA.

Chisci, L., Garulli, A. and Zappa, G. (1996). Recursive state bounding by parallelotopes, *Automatica* **32**(7): 1049–1055.

Di Francesco, G. and Mattei, M. (2015). Modeling and incremental nonlinear dynamic inversion control of a novel unmanned tiltrotor, *Journal of Aircraft* pp. 1–14.

Donadel, R. (2015). *Modeling and control of a tiltrotor unmanned aerial vehicle for path tracking*, Master's thesis, Federal University of Santa Catarina.

Donadel, R., Raffo, G. V. and Becker, L. B. (2014). Modeling and Control of a Tiltrotor UAV for Path Tracking, *Proc. of the 19th IFAC World Congress*, pp. 3839–3844.

Jazar, R. N. (2010). *Theory of applied robotics: kinematics, dynamics, and control*, Springer Science & Business Media.

Johnson, M. A. and Grimble, M. J. (1987). Recent trends in linear optimal quadratic multivariable control system design, *IEE Proceedings D*, pp. 53–71.

Kühn, W. (1998). Rigorously computed orbits of dynamical systems without the wrapping effect, *Computing* **61**(1): 47–67.

Le, V. T. H., Stoica, C., Alamo, T., Camacho, E. F. and Dumur, D. (2013). Zonotopic guaranteed state estimation for uncertain systems, *Automatica* **49**(11): 3418–3424.

Moore, R. E., Kearfott, R. B. and Cloud, M. J. (2009). *Introduction to Interval Analysis*, Society for Industrial and Applied Mathematics, Philadelphia, PA, USA.

Raffo, G. V., Ortega, M. and Rubio, F. R. (2011). Nonlinear $\mathcal{H}_\infty$ controller for the quad-rotor helicopter with input coupling, *Proc. of the 18th of the IFAC World Congress*, Vol. 18, pp. 13834–13839.